Orbital forcing of mid-latitude southern hemisphere glaciation since 100 ka, inferred from cosmogenic nuclide ages of moraine boulders from the Cascade Plateau, southwest New Zealand

Rupert Sutherland

GNS Science, PO Box 30-368, Lower Hutt, NZ.

Kyeong Kim

Lunar and Planetary Laboratory, University of Arizona, Tucson, AZ 85721-0092, USA

Albert Zondervan

GNS Science, PO Box 30-368, Lower Hutt, NZ.

Mauri McSaveney

GNS Science, PO Box 30-368, Lower Hutt, NZ.

GSA Data Repository Item

Corresponding author: Rupert Sutherland, Email: r.sutherland@gns.cri.nz,

Tel: (+64 4) 570 4873, Fax: (+64 4) 570 4603

PHYSIOGRAPHY AROUND THE CASCADE VALLEY

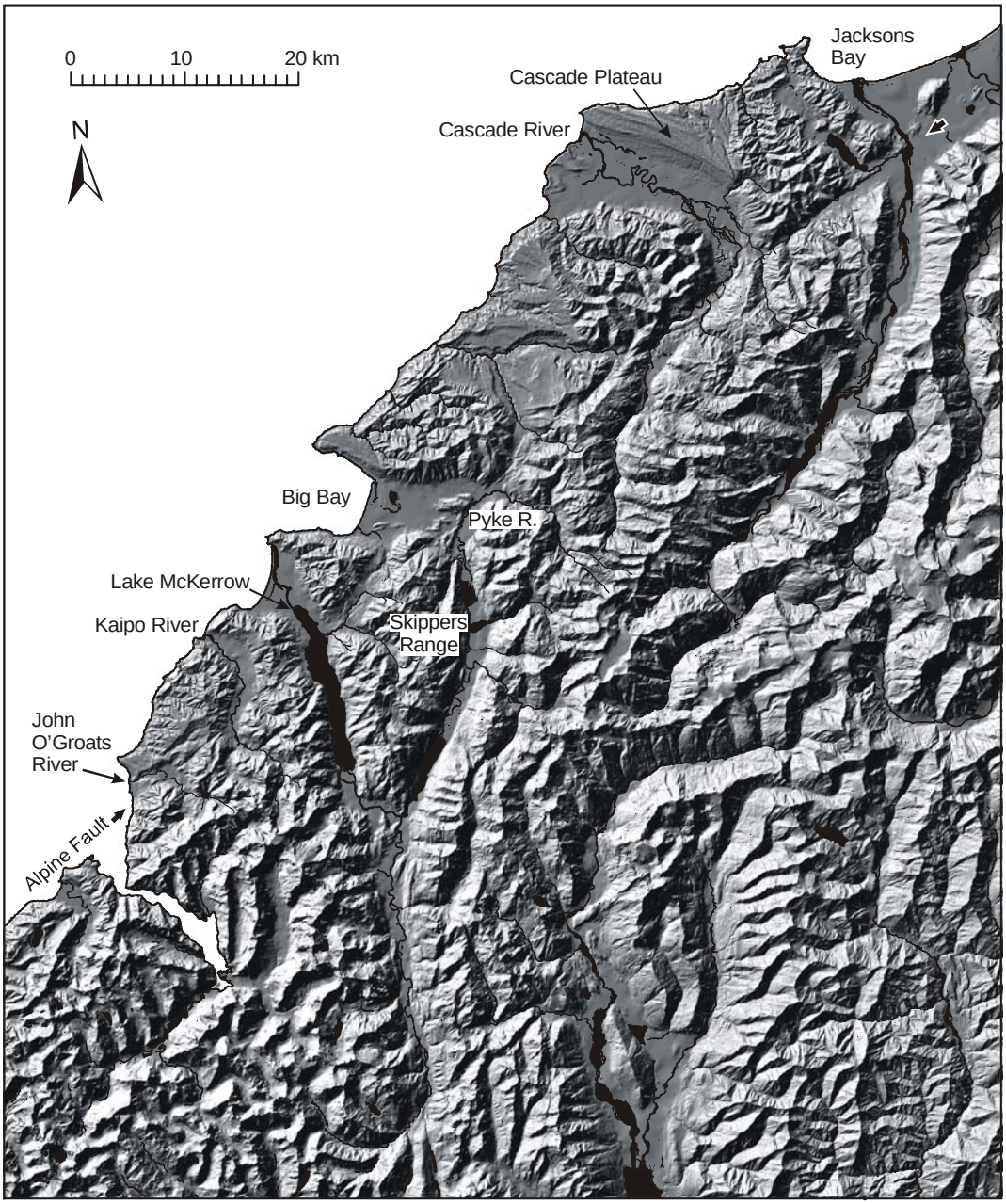

Figure DR1. Topography of the study region illuminated from the northwest (derived from NZMS 260 data). The Alpine fault offsets moraines or glacial morphology in almost every valley it crosses (Sutherland et al., 2006).

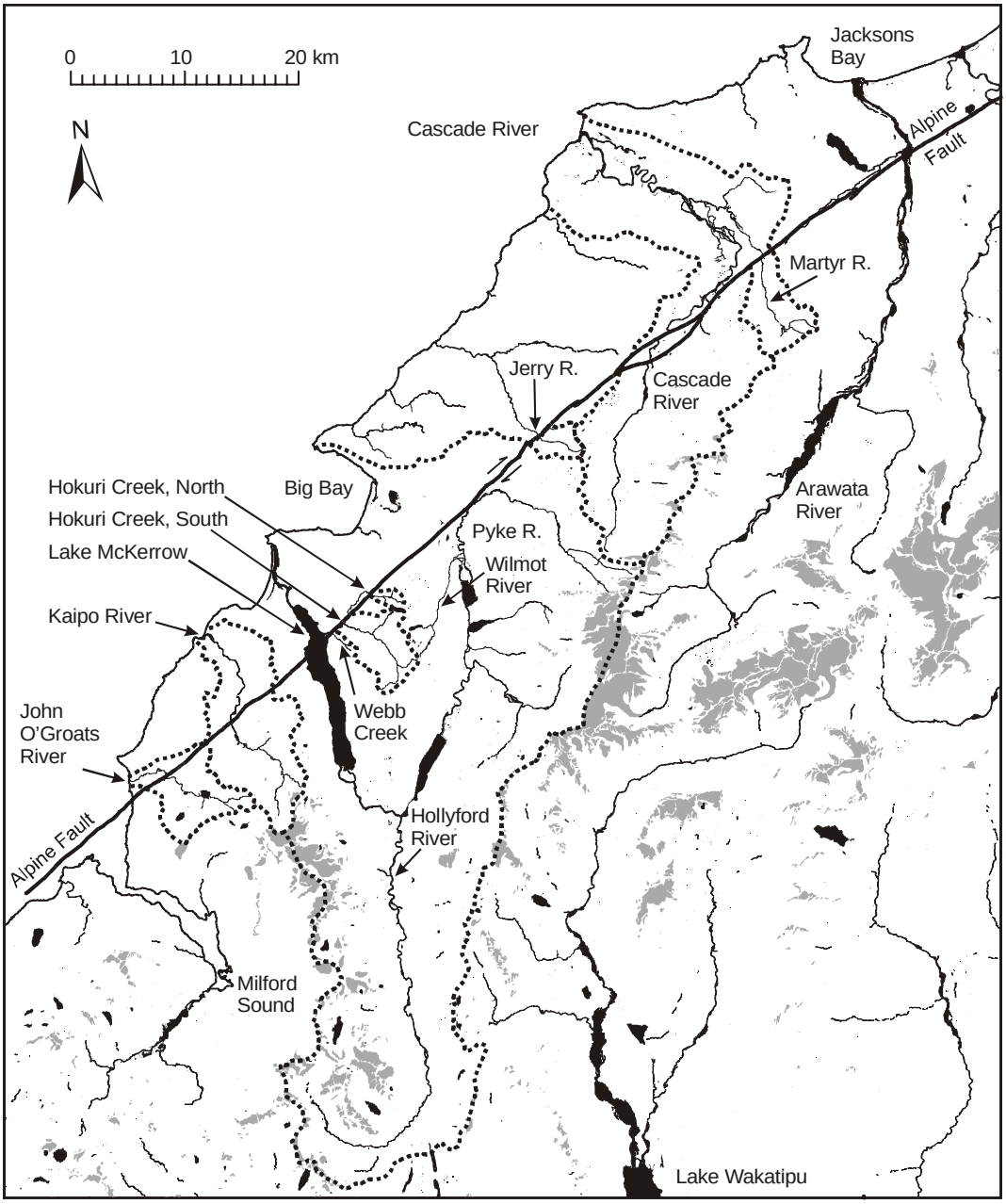

Figure DR2. Catchment boundaries (bold dotted lines) near to the Cascade valley. Areas of permanent snow and ice cover are shaded. Lakes and active river beds are shown black.

VALLEY HYPSOMETRY, PERMANENT SNOW COVER, AND GLACIER EQUILIBRIUM-LINE ALTITUDES

In order to better understand the context and implications of the Cascade valley moraine sequence, additional analysis is presented here of the valley and moraine geometries. Catchments within a relatively small area and with very similar local climatic conditions and facing directions display a range of surface areas and elevation differences (Figs. DR2 and DR3). There is a rapid reduction in the proportion of permanent snow cover for the highest catchments over an altitude range 2000-1500 m (Fig. DR4). Modern ELA height estimates in the range 1600-1800 m have been made over a number of years from a small number of existing glaciers (Fig. DR 4).

There is substantial debate about how cold conditions were during glacial maxima and we present one new dataset that is significant for this debate. The north branch of Hokuri Creek is a very small catchment with limited vertical extent, about 40 km southwest of the Cascade valley (Figs. DR2 and DR3). It is cut by the Alpine fault and has moraines that have been successively offset by c. 440, 1300, and 1900 m (Sutherland et al., 2006). It is possible to reconstruct the LGM extent of the former glacier quite accurately from observed moraine geometries, and calculate the paleo-ELA, given a range of assumed parameters (Fig. DR 4). By comparison with modern catchments, we predict about 800-1000 m suppression of the permanent snowline and note that the inferred paleo-ELA is about 1000 m lower than modern ELAs (Fig. DR4). The very small areal extent of the northern Hokuri catchment above 1000 m is significant, because it requires that the accumulation region of the former glacier was at least this low. Although we have not done any modelling of trade-offs between temperature and precipitation, it seems intuitive to us that it is not possible to generate a glacier with this geometry unless conditions were c. 5-6°C cooler than present. We identify the glaciated catchment geometry as being one end-member of the range available for testing hypotheses of past temperature and precipitation in western South Island.

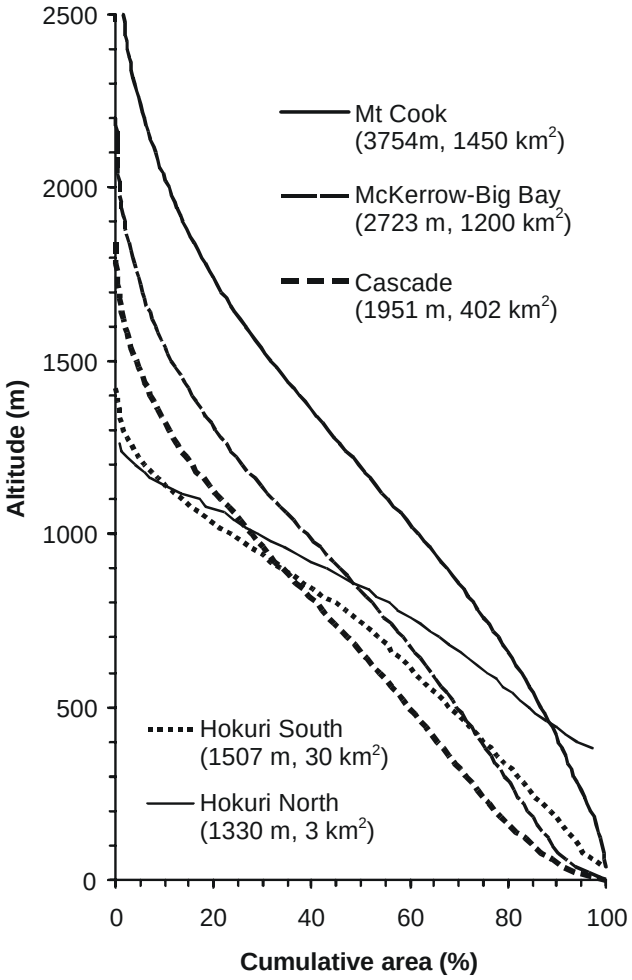

Figure DR3. Area-altitude relationship for: the Mount Cook region between the Alpine Fault and main drainage divide; the McKerrow-Big Bay catchment, which Hokuri Creek is a tributary within; the Cascade valley; and two branches of Hokuri Creek. Maximum peak heights and total surface area are reported in brackets.

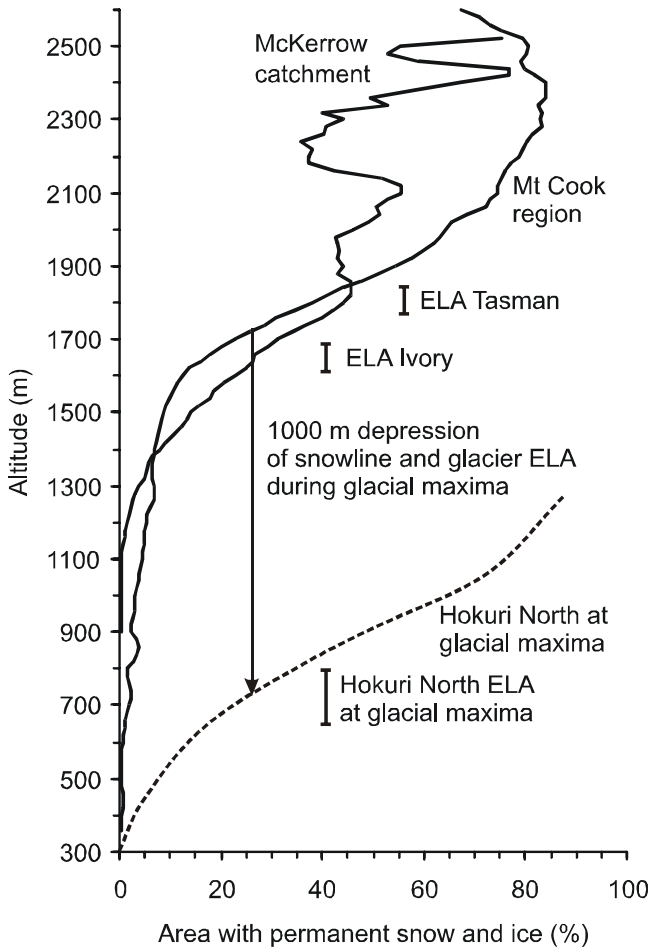

Figure DR4. Present percentage of permanent snow and ice cover for catchments flanking the western side of Mount Cook and the McKerrow catchment, of which Hokuri Creek is a tributary (solid lines). Data from digital analysis of NZMS 260 topographic map series. Contemporary equilibrium-line altitudes (ELAs) shown for the Ivory and Tasman glaciers (Dyurgerov, 2002). Reconstructed snow and ice cover for the north branch of Hokuri Creek is shown dashed and the range of ELA allowable for the paleo Hokuri glacier was calculated (Benn and Gemmell, 1997) using reconstructed glacier hypsometry and varying unknown parameters within a reasonable range.

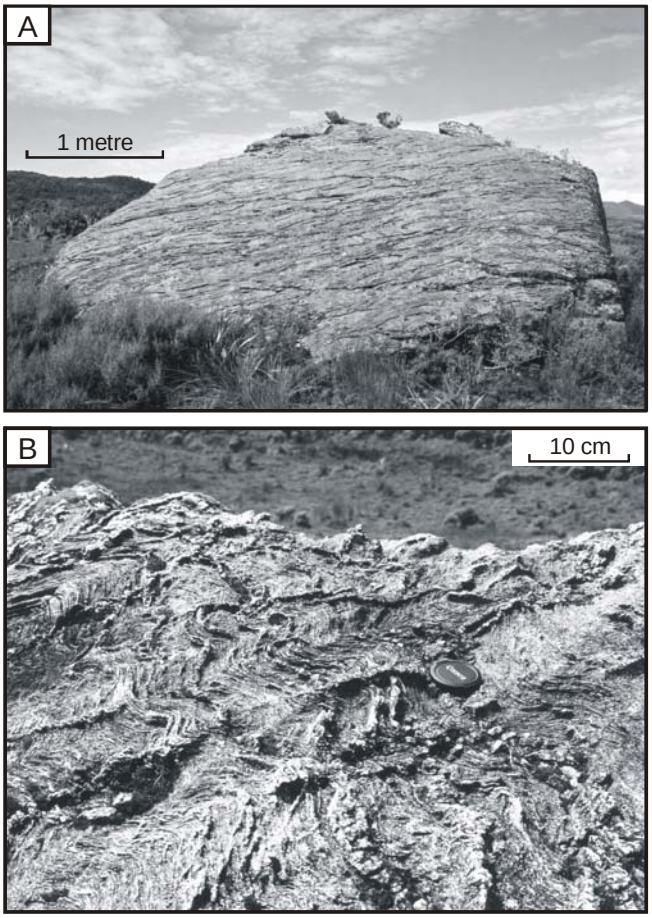

Figure DR5. A. Typical schist boulder embedded in moraine (sample 17); note loose fragment 20 cm thick on right edge of top surface. B. Quartz veining on top surface of schist boulder (sample 15).

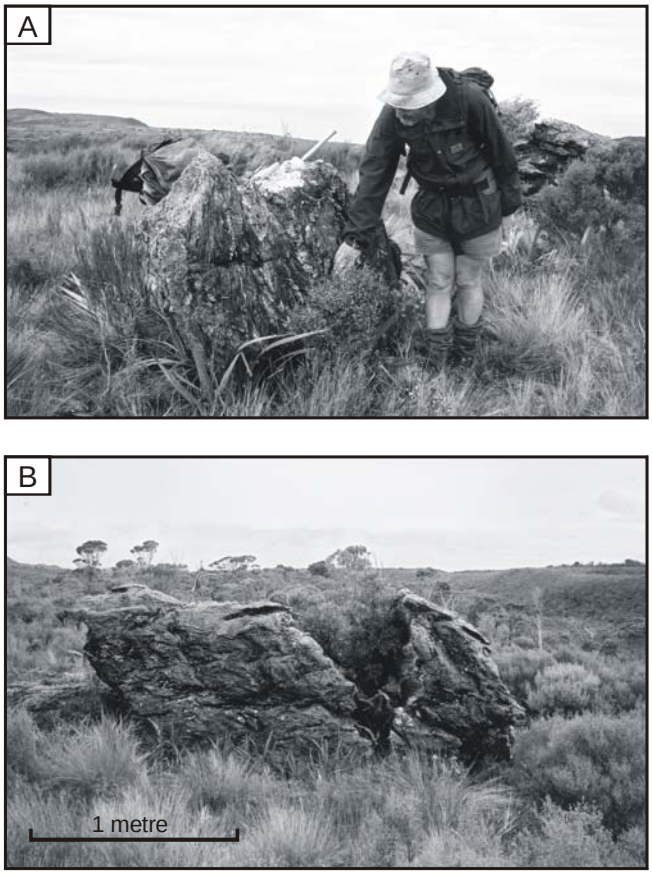

Figure DR6. A. Sample 9 has an anomalously young age and is from a relatively small boulder that may have rotated or/and have had fragments removed from the upper surface, or previously have been buried. B. Example of a boulder that has clearly fragmented (not sampled).

COSMOGENIC DATA AND AGE CALCULATION

TABLE DR1. SAMPLE LOCATIONS

Sample	X	Y
1	2147700	5675900
2	2147700	5675900
3	2147700	5675900
4	2148000	5676200
5	2148100	5676100
6	2148400	5675800
7	2148200	5676700
8	2148200	5676700
9	2148200	5676700
10	2148300	5677000
11	2148200	5677100
12	2148200	5677100
13	2143800	5676500
14	2143800	5676500
15	2143800	5676600
16	2143900	5676900
17	2144100	5676800
18	2144500	5676600
19	2145800	5677000
20	2145800	5677000

New Zealand Map Grid coordinates

TABLE DR2. ANALYTICAL RESULTS AND EXPOSURE AGES

Sample number	Altitude	^{10}Be surface production rate	AMS code (blank)	^{10}Be/^{9}Be	^{10}Be concentration	Age
	(m)	(atom g^{-1} yr^{-1})		(10^{-15})	(10^{4} atom g^{-1})	(^{10}Be ka)
13	215	6.11	Be-1773 (2)	110 ± 9	10.9 ± 1.1	18.7 ± 1.9
14	215	6.11	Be-1774 (2)	87 ± 8	8.1 ± 1.0	13.8 ± 1.7
15	225	6.17	Be-1775 (2)	122 ± 13	12.0 ± 1.5	20.4 ± 2.6
16	245	6.28	Be-1776 (2)	125 ± 8	12.7 ± 1.1	21.1 ± 1.8
17	250	6.31	Be-1777 (2)	123 ± 8	12.3 ± 1.0	20.4 ± 1.7
18	255	6.34	Be-1778 (3)	122 ± 8	11.3 ± 1.0	18.6 ± 1.7
19	345	6.87	Be-1779 (3)	109 ± 9	14.7 ± 1.6	22.4 ± 2.5
20	345	6.87	Be-1780 (3)	96 ± 7	11.4 ± 1.2	17.3 ± 1.9
1	390	7.15	Be-1764 (1)	354 ± 15	39.2 ± 1.8	57.8 ± 2.7
2	390	7.15	Be-1765 (1)	210 ± 11	21.8 ± 1.3	31.9 ± 2.0
3	390	7.15	Be-1766 (1)	315 ± 15	34.5 ± 1.8	50.8 ± 2.7
4	390	7.15	Be-1767 (1)	693 ± 19	53.3 ± 1.6	79.0 ± 2.4
5	395	7.19	Be-1768 (1)	194 ± 10	20.3 ± 1.2	29.5 ± 1.8
6	405	7.25	Be-1943 (4)	995 ± 24	53.0 ± 1.4	77.5 ± 2.1
7	370	7.03	Be-1769 (1)	467 ± 15	52.4 ± 1.8	79.0 ± 2.8
8	370	7.03	Be-1770 (1)	471 ± 29	53.0 ± 3.4	79.9 ± 5.2
9	370	7.03	Be-1944 (4)	399 ± 13	21.0 ± 0.8	31.2 ± 1.3
10	360	6.97	Be-1771 (2)	516 ± 17	76.3 ± 2.7	117.1 ± 4.2
11	355	6.94	Be-1945 (4)	552 ± 15	27.6 ± 0.9	41.8 ± 1.4
12	355	6.94	Be-1772 (2)	351 ± 24	52.1 ± 3.8	79.7 ± 5.8
			Be-1761 (= blank-1)	21 ± 3		
			Be-1762 (= blank-2)	18 ± 3		
			Be-1763 (= blank-3)	21 ± 4		
			Be-1946 (= blank-4)	6 ± 9		

Samples given in order of ascending depositional age, with moraine boundaries indicated by dashed lines. Chemistry blanks have been subtracted. Uncertainties reported are one standard deviation.

The altitude and geomagnetic-latitude scaling model of Stone (Stone, 2000), with a high-latitude sea-level production rate of 5.1 atom (g SiO_2)$^{-1}$ yr^{-1}, was used to calculate the production rate of ^{10}Be in quartz at the sampling locations, assuming maximum solid angle to the open sky and no attenuation by any material.

All samples were processed and measured via Accelerator Mass Spectrometry (AMS) at the GNS' National Isotope Centre, with the exception of samples 6, 9, and 11, which were submitted for wet chemistry at PrimeLab, Purdue University (Indiana, USA). Blanks 1-3 were produced at GNS and blank 4 at PrimeLab. Column 5 is the result of the AMS measurements on samples and blanks.

The reduction in ^{10}Be production rate across the depth interval of sampling, relative to the production rate at the surface, was calculated using an exponential expression for attenuation of fast neutrons, with attenuation length 165 g cm^{-2} and average rock density 2.65 g cm^{-3}. All samples were taken from a 0-5 cm depth interval relative to the present-day surface and assumed to have been exposed with this geometry since moraine deposition, and for there to have been zero initial ^{10}Be concentration. See main text for discussion of the exposure model and other assumptions used to calculate the age.

Uncertainties are one standard deviation and include uncorrelated uncertainties: known isotope measurement uncertainties for the sample and blank; a 1 cm uncertainty in sample thickness; and a 0.05 g cm^{-3} uncertainty in sample density.

STRATIGRAPHIC CORRELATION

TABLE DR3. CORRELATION BETWEEN REVISED GLACIAL STRATIGRAPHY OF THE CASCADE VALLEY AND OTHER GLACIAL UNITS IN SOUTHWEST NEW ZEALAND

Age (cal ka)	Cascade	Cascade*	Aurora Cave	Mt. Cook	N Westland
11.5-13	CA5	C5-3	Aurora-1	Waiho	
18-15	CA5	C5-2	Aurora-2	M6	K3
19-23	CA4	C4-1, C4-2, C5-1	Aurora-3	M5	K2-2
40-41			Aurora-4	M4b?	
46-48			Aurora-5	M4a?	
58-65	CA3	C4-1	Aurora-6	M3?	K2-1?
75-83	CA3	C3-3,C4-1		M2?	

After (Almond et al., 2001; Denton and Hendy, 1994; Suggate, 1990; Suggate and Waight, 1999; Williams, 1996).
*(Sutherland et al., 1995)

REFERENCES

Almond, P. C., Moar, N. T., and Lian, O. B., 2001, Reinterpretation of the glacial chronology of South Westland, New Zealand: New Zealand Journal of Geology and Geophysics, v. 44, no. 1, p. 1-15.

Benn, D. I., and Gemmell, A. M. D., 1997, Calculating equilibrium-line altitudes of former glaciers by the balance ratio method: a new computer spreadsheet: Glacial geology and geomorphology, http://ggg.qub.ac.uk/ggg/.

Denton, G. H., and Hendy, C. H., 1994, Younger Dryas age advance of Franz Josef Glacier in the Southern Alps of New Zealand: Science, v. 264, no. 5164, p. 1434-1437.

Dyurgerov, M., 2002, Glacier Mass Balance and Regime: Data of Measurements and Analysis, Occasional Paper: Boulder, USA, Institute of Arctic and Alpine Research, University of Colorado, 268 p.

Stone, J. O., 2000, Air pressure and cosmogenic isotope production: Journal of Geophysical Research, B, Solid Earth and Planets, v. 105, no. 10, p. 23,753-23,759.

Suggate, R. P., 1990, Late Pliocene and Quaternary glaciations of New Zealand: Quaternary Science Reviews, v. 9, no. 2-3, p. 175-197.

Suggate, R. P., and Waight, T. E., 1999, Geology of the Kumara-Moana area, scale 1:50 000, Institute of Geological and Nuclear Sciences Geological Map 24: Lower Hutt, New Zealand, Institute of Geological and Nuclear Sciences.

Sutherland, R., Berryman, K., and Norris, R. J., 2006, Quaternary slip rate and geomorphology of the Alpine fault: implications for kinematics and seismic hazard in southwest New Zealand: Geological Society of America Bulletin, v. 118, p. 464-474.

Sutherland, R., Nathan, S., Turnbull, I. M., and Beu, A. G., 1995, Pliocene-Quaternary sedimentation and Alpine Fault related tectonics in the lower Cascade Valley, South Westland, New Zealand: New Zealand Journal of Geology and Geophysics, v. 38, no. 4, p. 431-450.

Williams, P. W., 1996, A 230 ka record of glacial and interglacial events from Aurora Cave, Fiordland, New Zealand: New Zealand Journal of Geology and Geophysics, v. 39, no. 2, p. 225-241.